Characteristics of aerosol spectral optical depths over Manora Peak: A high-altitude station in the central Himalayas

Ram Sagar, Brijesh Kumar, and U. C. Dumka
State Observatory, Manora Peak, Nainital, India

K. Krishna Moorthy
Space Physics Laboratory, Vikram Sarabhai Space Centre, Trivandrum, India

P. Pant
State Observatory, Manora Peak, Nainital, India

Received 6 July 2003; revised 2 December 2003; accepted 10 December 2003; published 23 March 2004.

[1] We present, for the first time, spectral behavior of aerosol optical depths (AODs) over Manora Peak, Nainital, located at an altitude of ~2 km in the Shivalik ranges of the central Himalayas. The observations were carried out using a multiwavelength solar radiometer during January to December 2002. The main results of the study are extremely low AODs during winter, a remarkable increase to high values in summer, and a distinct change in the spectral dependencies of AODs from relatively steeper spectra during winter to shallower ones in summer. A comparison of the total optical depths of the nighttime measurements taken during the 1970s with the daytime values from the current study underlines the fact that loading of larger size particles during summer also occurred at that time, though less severely than it does today. During transparent days the AOD values usually lie below 0.08, while during dusty (turbid) days they lie between 0.08 and 0.69. The average AOD value during the winter, particularly in January and February, is $\sim 0.03 \pm 0.01$ at 0.5 μm. The mean aerosol extinction law at Manora Peak during 2002 is best represented by $0.10\lambda^{-0.61}$. However, during transparent days, which covers almost 40% of the time, it is represented by $0.02\lambda^{-0.97}$. This value of wavelength exponent, representing reduced coarse concentration and the presence of fine aerosols, indicates that the station measures aerosol in the free troposphere at least during part of the year. *INDEX TERMS:* 0305 Atmospheric Composition and Structure: Aerosols and particles (0345, 4801); 1610 Global Change: Atmosphere (0315, 0325); 1704 History of Geophysics: Atmospheric sciences; 1794 History of Geophysics: Instruments and techniques; *KEYWORDS:* aerosols, extinction

Citation: Sagar, R., B. Kumar, U. C. Dumka, K. K. Moorthy, and P. Pant (2004), Characteristics of aerosol spectral optical depths over Manora Peak: A high-altitude station in the central Himalayas, *J. Geophys. Res.*, *109*, D06207, doi:10.1029/2003JD003954.

1. Introduction

[2] Aerosols, both natural and anthropogenic, play an important role in atmospheric as well as astronomical sciences. They affect the atmospheric sciences by imparting radiative forcing and perturbing the radiative balance of the Earth-atmosphere system as well as by degrading the environment. To understand the effects of aerosols on our geo/biosphere systems, it is essential to characterize their physical, chemical, and optical properties at as many locations as possible because of the regional nature of their properties and the short lifetime [*Moorthy et al.*, 1999; *Satheesh et al.*, 2002]. This will also help in building up a comprehensive picture of global aerosol distribution and also their potential environmental impact. As most of the aerosol sources are of terrestrial origin, the variability of their properties will be very large close to the surface. At higher altitudes above the mixing region and in the free troposphere, the aerosol characteristics have a more synoptic perspective, would be indicative of the background level, and are useful to understand long-term impact. Such systematic measurements of aerosols at high altitudes are practically nonexistent in India.

[3] For ground-based optical astronomical observations also, precise knowledge of the Earth's atmospheric extinction behavior above a site is essential. Among many factors that cause extinction of light, the one due to scattering by aerosols is highly variable and controls the transparency as well as stability of the sky. Therefore characterization of atmospheric extinction at a site takes special importance in different atmospheric conditions like polluted or clear sky. Studying behavior of aerosol variation does help in evolving an average extinction law as well as indictating the quality of the site. Though some studies on the nighttime

0148-0227/04/2003JD003954$09.00

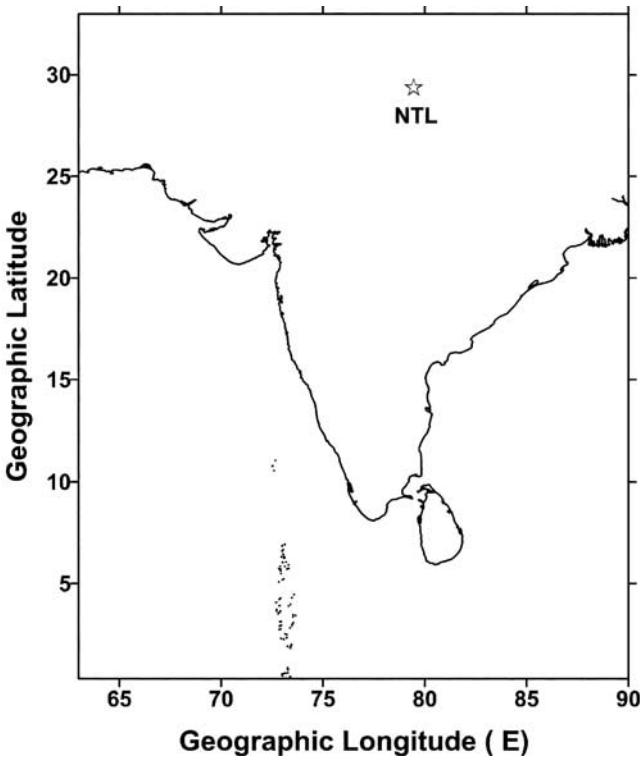

Figure 1. Geographical location of Manora Peak, Nainital (NTL), over the Indian subcontinent is given.

spectral behavior of aerosol optical depths (AODs) were done earlier [*Kumar et al.*, 2000], a multiwavelength study with narrowband filters has not been undertaken so far.

[4] Realizing the potential of and need for aerosol studies from both astronomical and atmospheric science perspectives, a program has been initiated at Manora Peak, Nainital, as a collaborative activity between the Space Physics Laboratory (SPL), Thiruvananthapuram, and the State Observatory, Nainital. Preliminary results, based on observations obtained during January to June 2002, are presented by *Sagar et al.* [2002]. In this paper, we present the results of extensive measurements of spectral AODs and deduced aerosol characteristics based on 1 year (January to December 2002) of observational data. The results are discussed and compared with similar measurements obtained during the nighttime in the 1970s.

2. Experimental Site, Observational Data, and Analysis

[5] The experimental site, Manora Peak, just southwest of Nainital, headquarters of the State Observatory, is located in the Shivalik ranges of the central Himalayas (latitude = 29°22′N, longitude = 79°27′E) at an altitude of ~2 km. The geographical location of the site over the Indian subcontinent is given in Figure 1. The daytime observations at Manora Peak on aerosols were made for 163 days during January to December 2002 with a multiwavelength solar radiometer (MWR) designed and developed by SPL. The instrument provides columnar total optical depths (TODs) at 10 narrowband wavelengths (FWHM of 6 to 10 nm, at different wavelengths) centered at 0.38, 0.40, 0.45, 0.50, 0.60, 0.65, 0.75, 0.85, 0.935, and 1.025 μm by making continuous spectral extinction measurements of directly transmitted solar radiation. The instrument works on the principle of a filter wheel radiometer [*Shaw et al.*, 1973] and has a field of view <2°. More details as to the instrument and the principle of data reduction and error budget are described by *Moorthy et al.* [1999, 2001]. Manora Peak, being a high-altitude station and experiencing very low AODs for a considerable portion of the year, meets the requirement for accurate calibration of the Sun photometer [*Shaw*, 1976].

[6] The observed flux, $F(\lambda, z)$, of the Sun at zenith distance, z, suffers extinction due to the Earth's atmosphere. It is proportional to $e^{-\tau_\lambda M(z)}$, where τ_λ is the columnar TOD of the Earth's atmosphere at wavelength λ and $M(z)$ is the relative air mass at z and is estimated following the general expression given by *Kondratyev* [1969]. As the output V_λ of the MWR at any wavelength is directly proportional to $F(\lambda, z)$, a least squares linear fit between the natural logarithm of V_λ and the corresponding relative air mass is used to estimate τ_λ following the so-called "Langley plot" method [*Shaw*, 1976]. Contributions toward τ_λ are due to scattering by air molecules ($\tau_{R\lambda}$) and aerosols ($\tau_{p\lambda}$) and due to gaseous absorption ($\tau_{\alpha\lambda}$). The $\tau_{\alpha\lambda}$ consists of molecular absorption due to ozone ($\tau_{oz\lambda}$), water vapor ($\tau_{w\lambda}$), and other gases such as NO_2. The $\tau_{R\lambda}$ values are estimated analytically using model/reference atmosphere profiles given by *Sasi and Sen Gupta* [1979]. They are 0.361, 0.291, 0.179, 0.116, 0.055, 0.040, 0.022, 0.014, 0.009, and 0.006, respectively, at the wavelengths under consideration. The ozone absorption mainly contributes in the Chappuis bands centered at 0.575 μm [*Gutiérrez-Moreno et al.*, 1982]. The significant values of $\tau_{oz\lambda}$ are 0.008, 0.032, and 0.017 at λ = 0.5, 0.6, and 0.65 μm, respectively, and zero at other wavelengths. There is also a weak absorption by NO_2 at wavelengths below 0.45 μm. The typical value of optical depth due to this is ~0.006 [*Tomasi et al.*, 1985]. The $\tau_{w\lambda}$ at affected wavelengths is determined following *Nair and Moorthy* [1998] using MWR measurements at 0.935 μm.

2.1. Daytime MWR Measurements

[7] The MWR data obtained during the study period have been analyzed as described above. On certain days, the Langley plots revealed occurrence of different least squares linear fit to the data with distinctly different slopes for the forenoon (FN) and afternoon (AN) parts of the same day implying different τ_λ. The MWR data are therefore analyzed separately considering the FN and AN parts of the data as two independent sets. A consolidated log of the data

Table 1. Observing Log of the Daytime Aerosol Measurements

		Data Sets		
Month (2002)	Days	Forenoon	Afternoon	Total
Jan.	12	11	06	17
Feb.	11	11	02	13
March	21	21	16	37
April	21	19	13	32
May	10	9	03	12
June	07	06	02	08
Sept.	05	05	00	05
Oct.	25	25	10	35
Nov.	27	27	20	47
Dec.	24	19	16	35
Total	163	153	88	241

thus analyzed is presented in Table 1. In all, 241 data sets, obtained on 163 days of the year 2002, have been analyzed. The data sets are spread over all months of the year except for July and August with maximum of 47 and minimum of 5 data sets for the months of November and September 2002, respectively (see Table 1). The complete absence of data in July and August and fewer observations in June and September are due to the highly cloudy sky conditions prevailing over the site, associated with the Indian summer monsoon [*Asnani*, 1993]. The values of $\tau_{p\lambda}$ ($= \tau_\lambda - \tau_{R\lambda} - \tau_{\alpha\lambda}$) at the wavelengths under study for each data set are given in Table A1 of the auxiliary material[1]. Filters at λ = 0.40 and 0.60 μm could be installed only on 11 October 2002 and 10 December 2002, respectively. The number of data sets at these wavelengths is therefore smaller. However, they will not affect the conclusions drawn in this paper.

[8] In order to check the stability and the quality of data obtained from MWR instrument, we study intercepts of all the Langley plots (i.e., $\ln(V_\lambda)$ values at zero air mass) against time for filters at 0.38, 0.5, and 0.75 μm. The distribution of the corresponding data points are best represented by mean ± standard deviation of 1.18 ± 0.08, 1.20 ± 0.06, and 0.78 ± 0.05, respectively. The overall errors in the measurements of $\tau_{p\lambda}$ at any wavelength are given as $\sigma^2_{\tau_{p\lambda}} = \sigma^2_{\tau_\lambda} + \sigma^2_{\tau_{R\lambda}} + \sigma^2_{\tau_{\alpha\lambda}}$. The σ_{τ_λ} arises because of 1-s resolution in time for air mass calculation, the statistical errors in regression analysis, and the errors due to variation in the Langley intercepts. All these added together contribute <0.02. The error in $\sigma_{\tau_{R\lambda}}$ arises because of the atmosphere models considered, and it may vary by 1%. The $\sigma_{\tau R\lambda}$ values will therefore be <0.01. Ozone models also vary, which may contribute an uncertainty of 0.003 at wavelengths between 0.5 to 0.65 μm. The AODs may therefore have a maximum uncertainty of ~0.03 at the wavelengths under consideration.

2.2. Nighttime Measurements

[9] As a part of optical astronomical observations, the nighttime values of τ_λ were determined on 13 nights during 1970 to 1978 at 20 wavelengths ranging from 0.34 μm to 0.76 μm with a bandwidth of 5 nm (details are given in Table A2 of the auxiliary material[1]). The observations were obtained using 0.5 and 1 m size optical telescopes along with a star photometer. Further details of the observations and measurements are given by *Kumar et al.* [2000]. The τ_λ measurements can therefore be considered monochromatic and hence similar to the MWR observations. The accuracy of the nighttime measurements lies between 0.01 and 0.02 per air mass, being maximum at a wavelength slightly shorter than 0.4167 μm. It is thus similar to that of the daytime measurements. They can therefore be compared with the daytime MWR measurements for the study of spectral properties but not for the study of monthly variations because of the rather small database.

3. Results and Discussion

3.1. Temporal Variation of AODs

[10] Figures 2a and 2b show the temporal variations of AODs at the representative wavelength, 0.5 μm, and water vapor content, respectively. During 15 June to 15 September, no AODs observations could be taken because of the reasons discussed above. The data cover the range from excellent "coronal" days, where $\tau_{p\lambda}$ is very low (<0.1), to "absorbent" (with high $\tau_{p\lambda} > 0.4$) days, where summer dust from the adjoining plain areas is present above the site. Fortnightly or the monthly means along with minimum and maximum AOD values at all the MWR wavelengths during the study period are given in Table A3, again in the auxiliary material[3] because of its large size. In order to have statistically significant results, monthly means are taken if the number of data sets in a month is <20. A plot of these at 0.5 μm are also shown by the solid lines in Figure 2a. Figures 2b–2f show the mean value of columnar water vapor content W (g/cm^2), relative humidity (%), rainfall (cm), wind speed (m/s), and wind direction (degrees). These plots clearly show correlated variations. The monthly mean values of AOD at 0.5 μm and W, along with the respective standard deviations and ranges, are given in Table 2. The average values of $\tau_{p\lambda}$ at 0.50 μm are ~0.03 ± 0.01 during January and February, between 0.06 and 0.11 during September to 15 December, and in the range of 0.16 to 0.36 during 15 March to June. The AOD values are thus lowest during winter and postmonsoon (January to mid-March and October to December). However, they increase rather rapidly, attaining a peak value during summer (April to June), following a transition in the month of March. The next transition from peak to low might be occurring during the rainy months when the MWR data are absent.

[11] The monthly variation of major surface meteorological parameters at the site is also shown in Figure 2 to study its possible effects on aerosols. The water vapor content, W, is below 0.2 g/cm^2 for 80% of the measurements with a mean value of 0.1 g/cm^2, implying a dry environment, while it is greater than 0.2 g/cm^2 mostly in summer and in the month of October. An increase in W (when higher than 3 g/cm^2) is known to cause a nonlinear increase in AOD at all wavelengths covered by MWR [*Nair and Moorthy*, 1998; *Moorthy et al.*, 2001]. As the values of W are very low at the site, the temporal variations in W and AOD are quite similar (see Figure 2), with the only exception being for the month of October, where AODs are small despite large (>0.2 g/cm^2) values of W. This indicates that the variations in AOD and W are brought about mostly by the same processes related to local and synoptic changes in the meteorological conditions. The rainfall climatology shows that the rainfall is highest during July to September (accounting for about 68% of the annual rainfall)with very little rain during the period March to middle of June (when it is only 12% of the annual). Figures 2e and 2f give the mean wind speed and wind direction of arrival recorded during 2002 at the site. The arrival wind direction is indicated in degrees with 0°, 90°, 180°, and 270° corresponding to the north, east, south, and west directions, respectively. The mean wind speed, ~2 ms^{-1} during winter, doubles during premonsoon. During the same period the mean arrival wind direction gradually shifts from southerly to westerly. For the location of the site this would mean a shift in the air mass from the southern (with respect to the station) Indian plains in winter to the western arid land mass during summer, when the winds arrive from the vast arid regions of northwest India and regions lying farther to

[1]Auxiliary material is available at ftp://ftp.agu.org/apend/jd/2003JD003954.

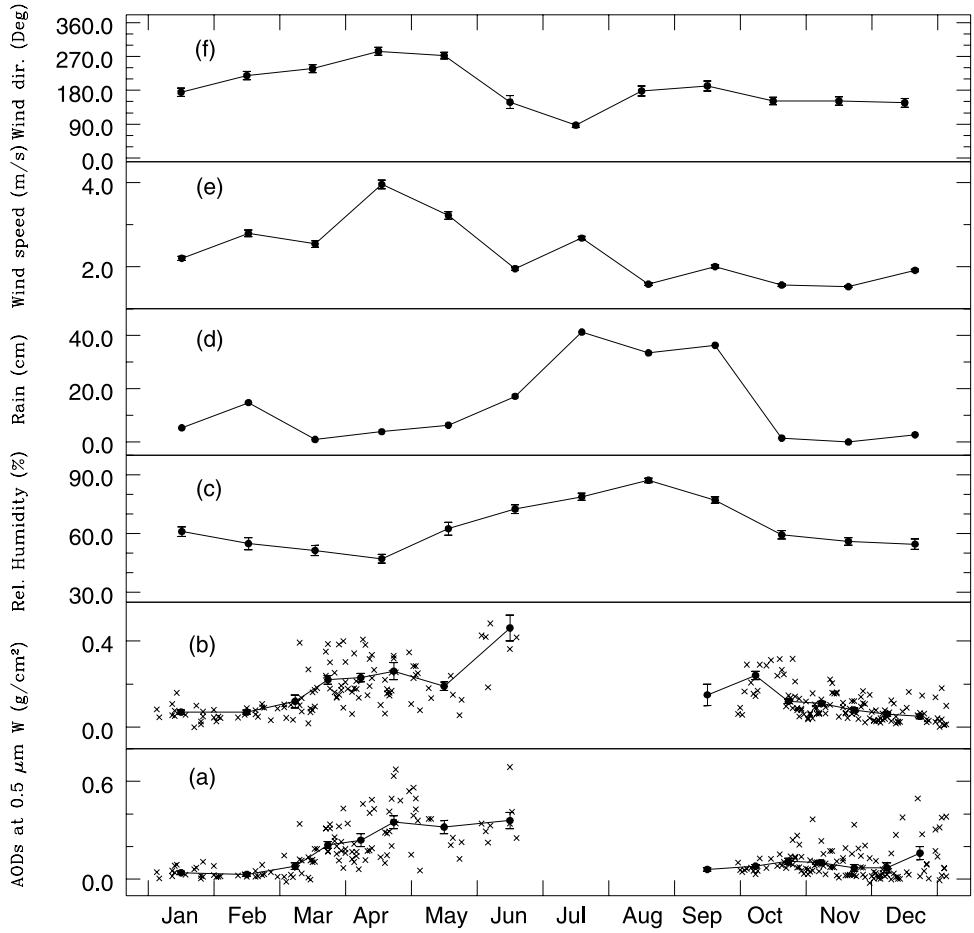

Figure 2. Temporal variations of the daytime AOD at 0.5 μm during the year 2002 are shown in Figure 2a. Figure 2b shows the corresponding variations in water vapor content. The fortnightly/monthly mean values are also plotted in these panels (see text). Monthly variations of relative humidity, rainfall, wind speed, and mean arrival wind direction are shown in Figures 2c, 2d, 2e, and 2f, respectively.

its west. This change in the air mass type is obviously mostly responsible for the rapid buildup in the AOD over the station after March as the arid air mass is known to transport large amounts of desert/mineral aerosols from the west Asian and Indian deserts, lying to the west/southwest of this station. The role of wind-blown dust from the deserts in increasing turbidity over northern Indian regions has been suggested earlier by *Mani et al.* [1969]. Recently, on the basis of satellite data analysis, *Li and Ramanathan* [2002] have also shown the eastward transport of west Asian deserts aerosols across the northern Arabian Sea toward the west coast of India. Thus the observed sharp increase in the AOD from the middle of March is mostly attributed to this. In addition to the advection by air mass, the increased solar heating of the land mass over the lower plains adjacent to the site during the summer season would result in increased convective mixing and elevation of the boundary layer aerosols. This would also contribute to the increase in AOD over the site during the summer season.

[12] The AOD values for each month as well as for the entire year are grouped together and the percentage fre-

Table 2. Monthly Mean AODs (at 0.5 μm), Water Vapor Content, and Aerosol Wavelength Exponent[a]

	AODs at 0.5 μm			W, g cm^{-2}			α		
Month (2002)	Min	Mean ± SD	Max	Min	Mean ± SD	Max	Min	Mean ± SD	Max
Jan.	0.00	0.04 ± 0.01	0.11	0.00	0.06 ± 0.01	0.16	1.55	1.90 ± 0.27	2.61
Feb.	0.01	0.03 ± 0.01	0.09	0.03	0.07 ± 0.01	0.11	0.78	1.52 ± 0.18	2.52
March	−0.01	0.16 ± 0.02	0.44	0.02	0.18 ± 0.02	0.40	0.17	1.08 ± 0.09	1.76
April	0.06	0.29 ± 0.03	0.67	0.06	0.24 ± 0.02	0.72	0.01	0.70 ± 0.16	1.30
May	0.05	0.32 ± 0.04	0.56	0.05	0.19 ± 0.02	0.28	0.42	0.68 ± 0.16	1.35
June	0.22	0.36 ± 0.05	0.69	0.19	0.46 ± 0.06	0.74	0.21	0.47 ± 0.52	0.91
Sept.	0.05	0.06 ± 0.01	0.10	0.06	0.13 ± 0.04	0.29	0.40	1.08 ± 0.26	1.46
Oct.	0.03	0.11 ± 0.01	0.37	0.04	0.15 ± 0.01	0.32	0.37	1.20 ± 0.11	2.22
Nov.	−0.02	0.08 ± 0.01	0.33	0.02	0.09 ± 0.01	0.22	0.40	1.45 ± 0.07	2.81
Dec.	−0.01	0.12 ± 0.02	0.50	0.00	0.06 ± 0.01	0.18	0.10	1.26 ± 0.13	2.76

[a]W, water vapor content; α, aerosol wavelength exponent. SD, standard deviation; min, minimum; max, maximum.

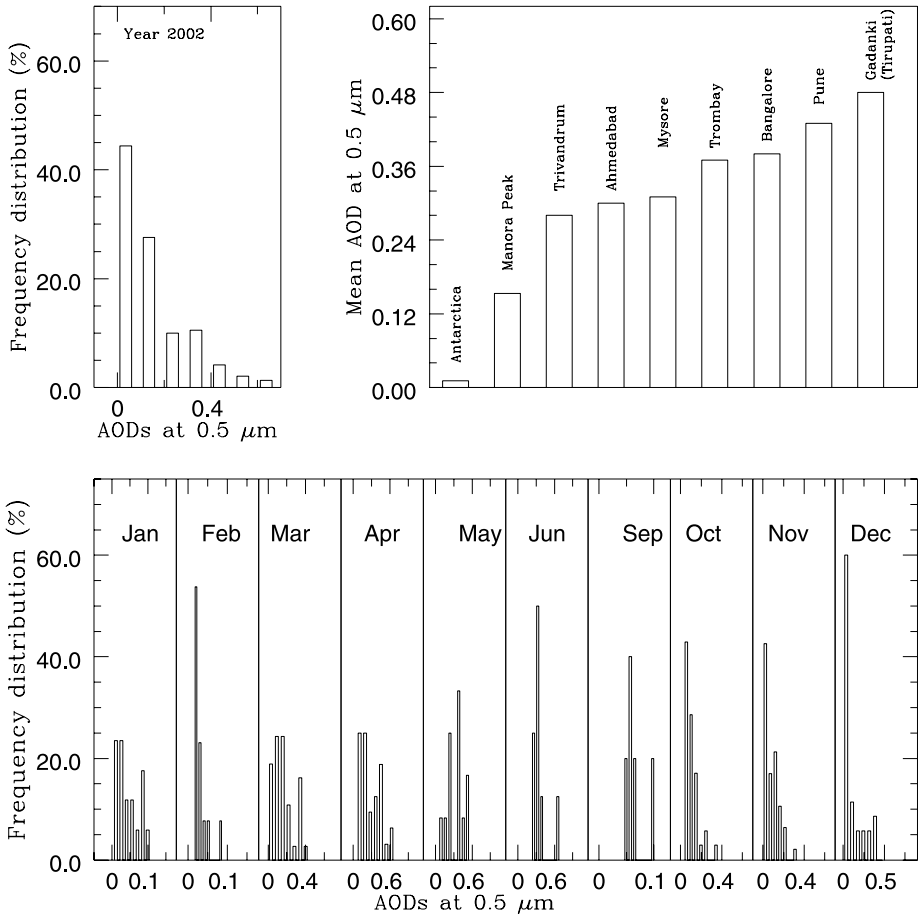

Figure 3. Lower panels show monthly variation of frequency distribution of AODs at 0.5 μm during the year 2002, while the upper panels show their yearly frequency distribution and comparison with those at Antarctic and other Indian locations.

quency distributions for different $\tau_{p\lambda}$ ranges have been plotted in Figure 3. Here again, it is observed that day-to-day variability is maximum during April, May, and June. The distributions are highly skewed in winter months, while in summer they tend to be more symmetric. These distributions support the conclusions drawn earlier.

3.2. Comparison of AODS With Other Locations

[13] The yearly mean values of AODs at the site are 0.180, 0.174, 0.163, 0.153, 0.137,0.130, 0.119, 0.110, 0.104, and 0.098, respectively, for the 10 wavelengths under investigation. However, it may be noted that the corresponding mean AOD values are 0.043, 0.041, 0.036, 0.033, 0.028, 0.026, 0.022, 0.020, 0.018, and 0.017, respectively, during winter. The yearly mean $\tau_{p\lambda}$ values over Manora Peak, representative of the 10-month period during 2002, are higher than that observed over Antarctica during 3 months of the summer period [*Gadhavi and Jayaraman*, 2002], while the winter values are similar to the values recorded in the Antarctic environment (Figure 3). This indicates a very clean environment over Manora Peak at least during part of the year 2002. The yearly mean values of $\tau_{p\lambda}$ for Manora Peak are much lower than the average values observed over typical urban regions like Ahmedabad [*Ganguly et al.*, 2002], Trombay [*Sunny et al.*, 2002], Bangalore [*Babu et al.*, 2002], Gadanki [*Rao et al.*, 2002], and Pune [*Pandithurai et al.*, 2002] during the year 2002 (see Figure 3).On the basis of over 10 years of observations, *Moorthy et al.* [1999] have reported annual mean values of AOD at 0.5 μm as 0.28 for Trivandrum, 0.31 for Mysore, and 0.5 for Gadanki.

3.3. Spectral Variation of AODs

[14] The seasonal variations of the AOD spectral properties are plotted in Figure 4 (lower panel), grouped in winter, summer, and March (transition month as discussed earlier).The AODs are averaged during these periods. The vertical bars show the standard deviations. The properties of winter and summer aerosols are different, as can be seen from the variations of their λ dependence.

[15] To study the spectral differences as a function of $\tau_{p\lambda}$, we grouped all the data into three groups according to $\tau_{p\lambda}$ values at 0.5 μm. The groups are $\tau_{p\lambda} < 0.08$, $0.08 \leq \tau_{p\lambda} < 0.25$ and $\tau_{p\lambda} \geq 0.25$. The wavelength dependence of AOD for these groups is displayed in the middle panel of Figure 4. This clearly indicates the differences between the sizes of particles contributing to the AODs of different groups. The spectral variation of the group with the largest values of AOD corresponds to the summer period, as expected. However, the spectral variation of the group with the lowest AODs is not similar to the winter period.

[16] The upper panel of Figure 4 shows a comparison of TODs observed for the year 2002 with those measured

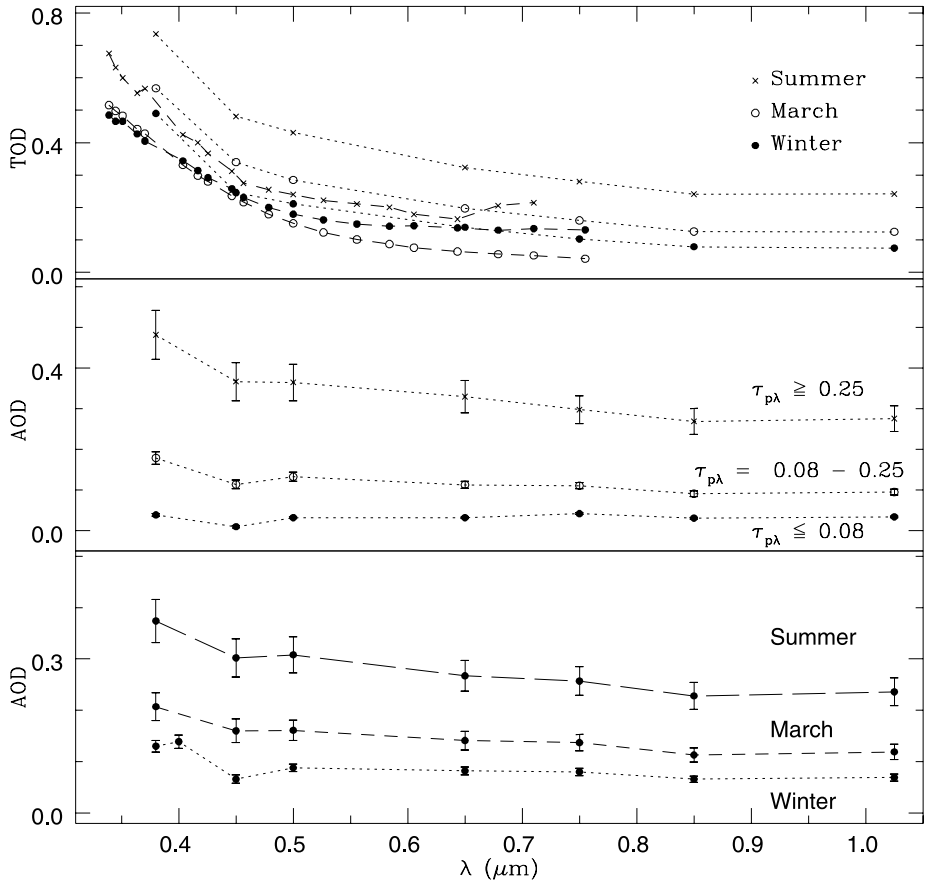

Figure 4. Lower panel shows spectral variation of daytime AODs during different seasons, while the middle panel displays the spectral variation of different $\tau_{p\lambda}$ at 0.5 μm. The upper panel compares the daytime as well as nighttime total optical depths, with dotted and dashed lines, respectively.

during nighttime in the seventies. In order to avoid crowding, the standard deviations are not plotted. The number of data sets is smaller for the nighttime measurements. Nevertheless, the summer-winter trend is apparent even in the nighttime in the seventies; however, the differences between the two values are not as high as they are for the year 2002 during daytime. This could be due to several reasons. It is possible that the general increase in AOD at some Indian stations reported by *Moorthy et al.* [1999] and *Satheesh et al.* [2002] might be contributing to an increase in AOD in the free troposphere, because of increased aerosol loading. Particularly in summer, another possibility is that the increased convective turbulence during premonsoon/summer months would be pumping in more surface level aerosols to higher altitudes, which would decrease in the nighttime because of the collapse in the boundary layer height. This would lead to higher AODs in the daytime. This effect could be more conspicuous at short wavelengths, as small particles can easily be lifted by turbulence. This aspect can be verified only by making both nighttime and daytime measurements during the same period.

[17] An interesting feature of the TODs, common to both the daytime and nighttime measurements, is their ultralow values for a few percent of the total measurements. The occurrence of these values is more prominent for the nighttime measurements during the 1970s, indicating a clearer atmosphere (see Figure 4, top panel). The lowest daytime TOD was obtained for the FN data set of 4 March 2002. The rain poured heavily previous to this day. Similarly, the log hints at ultraclear or pure skies on these dates. It may be noted that these ultralow values of TOD are generally obtained during November to March of the year between 0.34 and 0.45 μm and are more pronounced for nighttime measurements. At 0.36 μm the TOD values lower by ∼0.1 than expected from standard atmosphere models have also been obtained at other central Himalayan sites, e.g., at Devasthal (latitude = 29°22′N, longitude = 79°41′E, altitude = 2450 m) by *Mohan et al.* [1999] and at Hanle (latitude = 32°47′N, longitude = 78°58′E, altitude 4500 m) by *Parihar et al.* [2003] during nighttime measurements using broadband (half width ∼200 Å) filters. The occurrence of negative AODs mostly at shorter wavelengths may arise either because of changes in the climatological values of ozone column content at the central Himalayan sites or because of the use of a model atmosphere, such as that obtained from a tropical station by *Sasi and Sen Gupta* [1979]. Thus overestimation of Rayleigh and ozone corrections may result in the negative AODs. It could also be due to very high value of Rayleigh optical depth (∼90% of the TODs at these wavelengths) being subtracted from τ_λ. Also, the uncertainty of ±0.03 in AOD determination does cover most of these negative values; however, these

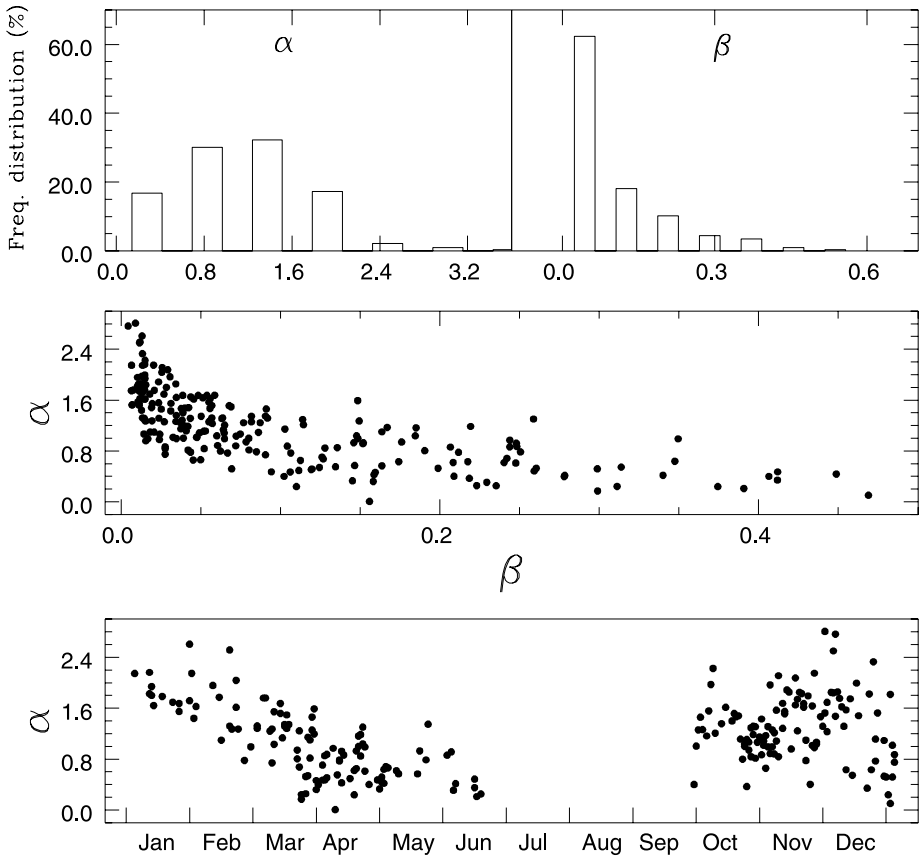

Figure 5. Variation of α with time is shown in the lower panel. A correlation between α and β and their frequency distributions over the entire period are presented in the other panels.

values may be used to constrain the existing models of standard Earth atmosphere for the Himalayan region.

3.4. Determination of Aerosol Properties/Angström Coefficients

[18] Following *Angström* [1961], the wavelength variation of AOD can be expressed as $\beta\lambda^{-\alpha}$, where β and α are the constants and vary widely. The wavelength exponent α is a measure of the relative dominance of fine, submicrometer-sized aerosols over the coarse aerosols while β is a measure of the total aerosol loading. A higher value of α signifies increased relative abundance of fine particles. The values of both α and β are determined from the individual data sets of the present MWR observations. The correlation of α with β is shown in the middle panel of Figure 5. We see that as β increases, α decreases (though the relation is not linear). This indicates that as the aerosol loading increases, the relative dominance of fine aerosol decreases. In other words, the increase in aerosol loading is due more to increase in coarse aerosol particles.

[19] Temporal variation of α is shown in Figure 5 along with the frequency distributions of both α and β. The monthly mean values of α along with the range are given in Table 2. The average value of α decreases systematically from January to March and remains at that level until June, while it shows large scatter during October to December with an increased average. Histograms indicate highly skewed distributions for β with most of the values <0.1, while α values have a wide Gaussian distribution with peak around 1 (see uppermost panel of Figure 5).

[20] We have also derived the values of α and β by fitting the aerosol extinction law in the mean values of AODs for different ranges of AODs and seasons as well as for the whole year. The values of β and α are 0.017 ± 0.005 and 0.97 ± 0.09 when AOD at 0.5 μm < 0.08, while the corresponding values for AOD ≥ 0.08 are 0.153 ± 0.005 and 0.54 ± 0.07, respectively. The values of β for the winter, March, and summer are 0.06 ± 0.01, 0.11 ± 0.01, and 0.22 ± 0.01, respectively, while the corresponding values of α are 0.72 ± 0.12, 0.54 ± 0.08, and 0.46 ± 0.07, respectively. The decrease in α signifies an increase in the relative abundance of coarse mode aerosols. For the entire data set, mean values of β and α are found to be 0.10 ± 0.01 and 0.61 ± 0.08, respectively. The mean value of α decreases from winter to summer, while during the same period, the β value is enhanced by a factor of 4. This observation is important for aerosol characterization at the site. During winter (when land temperatures are very low (0 to 19°C) and minimum solar zenith angle is $\geq 40°$) the surface convective (thermal) activities will be very weak. The observation site being at $\sim$2 km above MSL, well above the mixed layer, its environment will thus be free of all local contamination, and aerosol characteristics will pertain more closely to that of the free troposphere. In this region the dominating aerosols will be submicron-sized ones formed either in situ by secondary gas-to-particle conversion processes of the

precursors (which might be more anthropogenic and regional in nature). These fine aerosols would rapidly undergo size transformation by coagulation and condensation growth to accumulation size range. The aerosol size spectrum would thus be dominated by these particles, and hence the AOD spectra during winter would be steeper with a higher value of α and a low value of β. As the Sun enters the Northern Hemisphere, the surface heating increases, and there is a better exchange between the boundary layer and free troposphere because of increased convective mixing and the increase in the altitude extent of the convective boundary layer. This is conducive for the local aerosols (which are likely to have a large share of coarse particles) to impact the site. In addition to this, the arid aerosols, advected by the westerly winds, would also contribute to increased coarse particle abundance. As a result, the total aerosol loading and the share of coarse aerosol in it increases. This is reflected by the steady increase in β, the decrease in α, and the flattening of AOD spectrum. This continues until the monsoon rains intervene and remove the aerosols by scavenging.

4. Conclusions

[21] The main conclusions of our study are the following:

[22] 1. AODs over Manora Peak shows significant temporal variations during the year 2002. There is a remarkable increase in AOD from their very low values in winter to high values in summer. During the winter season, the AODs are of a magnitude comparable to the Antarctic environment, while during summer they are typical of continental regions.

[23] 2. During transparent days the AOD at 0.5 μm lies usually below 0.08, while during dusty days it lies between 0.08 and 0.69. The mean aerosol extinction law at the site during 2002 is best represented by $0.10\lambda^{-0.61}$. During transparent days, for 40% of the observable days, it is $0.02\lambda^{-0.97}$.

[24] 3. A comparison of the total optical depths of the nighttime measurements taken during the 1970s with the daytime measurements underlines the fact that summer sky pollution also occurred at that time, though less severely than it does today.

[25] 4. The water vapor content, W, lies <0.2 g/cm^2, for 80% of the clear days.

[26] **Acknowledgments.** The authors acknowledge the anonymous reviewers, whose useful comments have improved the paper substantially. We gratefully acknowledge the initiative and keen interest taken by R. Sridharan, Director, SPL, in this collaborative program. We also thank Wahab Uddin and the technical staff of the State Observatory, Nainital, for providing valuable help during observations and to the technical staff of SPL, Trivandrum, for installing the instrument at the site.

References

Angström, A. (1961), Techniques of determining the turbidity of the atmosphere, *Tellus*, *13*, 214–223.

Asnani, G. C. (1993), *Tropical Meteorology*, vol. 1, 603 pp., Indian Inst. of Trop. Meteorol., Pune.

Babu, S. S., S. K. Satheesh, K. K. Moorthy, and V. Vinoj (2002), Aerosol radiative forcing over land due to black carbon aerosols, *Bull. Indian Aerosol Sci. Technol. Assoc.*, *14*, 88–90.

Gadhavi, H., and A. Jayaraman (2002), Direct aerosol radiative forcing experiment over Antarctica, *Bull. Indian Aerosol Sci. Technol. Assoc.*, *14*, 40–42.

Ganguly, D., H. Gadhavi, and A. Jayaraman (2002), Pre-monsoon aerosol characteristics over Ahmedabad, *Bull. Indian Aerosol Sci. Technol. Assoc.*, *14*, 37–39.

Gutiérrez-Moreno, A., H. Moreno, and G. Cortés (1982), A study of atmospheric extinction at Cerro Tololo Inter-American observatory, *Publ. Astron. Soc. Pac.*, *94*, 722–728.

Kondratyev, K. Y. (1969), *Radiation in the Atmosphere*, 912 pp., Academic, San Diego, Calif.

Kumar, B., R. Sagar, B. S. Rautela, J. B. Srivastava, and R. K. Srivastava (2000), Sky transparency over Nainital: A retrospective study, *Bull. Astron. Soc. India*, *28*, 675–686.

Li, F., and V. Ramanathan (2002), Winter to summer monsoon variation of aerosol optical depth over the tropical Indian Ocean, *J. Geophys. Res.*, *107*(D16), 4284, doi:10.1029/2001JD000949.

Mani, A., O. Chacko, and S. Hariharn (1969), A study of Angström's turbidity parameters from solar radiation measurements in India, *Tellus*, *21*, 829–843.

Mohan, V., W. Uddin, R. Sagar, and S. K. Gupta (1999), Atmospheric extinction at Devasthal, Nainitald, *Bull. Astron. Soc. India*, *27*, 601–608.

Moorthy, K. K., K. Niranjan, B. Narasimhamurthy, V. V. Agashe, and B. V. K. Murthy (1999), Aerosol climatology over India. 1: ISRO GBP MWR network and database, *ISRO GBP SR–03-99*, Indian Space Res. Organ., Bangalore.

Moorthy, K. K., A. Saha, B. S. N. Prasad, K. Niranjan, D. Jhurry, and P. S. Pillai (2001), Aerosol optical depths over peninsular India and adjoining oceans during the INDOEX campaigns: Spatial, temporal, and spectral characteristics, *J. Geophys. Res.*, *106*, 28,539–28,554.

Nair, P. R., and K. K. Moorthy (1998), Effects of changes in the atmospheric water vapour content on the physical properties of atmospheric aerosols at a coastal station, *J. Atmos. Sol. Terr. Phys.*, *60*, 563–572.

Pandithurai, G., R. T. Pinker, and P. C. S. Devara (2002), Variability of climatically important aerosol optical properties over an urban tropical site as retrieved from sky radiometer observation, *Bull. Indian Aerosol Sci. Technol. Assoc.*, *14*, 19–22.

Parihar, P. S., D. K. Sahu, B. C. Bhatt, A. Subramaniam, G. C. Anupama, and T. P. Prabhu (2003), Night sky extinction measurements at the Indian Astronomical Observatory, Hanle, *Bull. Astron. Soc. India*, *31*, 453–454.

Rao, Y. J., P. C. S. Devara, A. K. Srivastava, S. Sonbawne, and Y. B. Kumar (2002), Lidar and radiometric observations of aerosols over Gadanki (13.8N, 79.2E), *Bull. Indian Aerosol Sci. Technol. Assoc.*, *14*, 23–26.

Sagar, R., B. Kumar, P. Pant, U. C. Dumka, K. K. Moorthy, and R. Sridharan (2002), Aerosol contents at an altitude of 2km in central Himalayas, *Bull. Indian Aerosol Sci. Technol. Assoc.*, *14*, 167–170.

Sasi, M. N., and K. Sen Gupta (1979), Scientific report, *ISRO VSSC SR 19*, 72 pp., Vikram Sarabhai Space Cent., Trivandrum, India.

Satheesh, S. K., V. Ramanathan, B. N. Holben, K. K. Moorthy, N. G. Loeb, H. Maring, J. M. Prospero, and D. Savoie (2002), Chemical, microphysical, and radiative effects of Indian Ocean aerosols, *J. Geophys. Res.*, *107*(D23), 4725, doi:10.1029/2002JD002463.

Shaw, G. E. (1976), Error analysis of multiwavelength Sun photometry, *Pure Appl. Geophys.*, *114*, 1–14.

Shaw, G. E., J. A. Regan, and B. M. Herman (1973), Investigations of atmospheric extinctions using direct solar radiation measurements made with a multiple wavelength radiometer, *J. Appl. Meteorol.*, *12*, 374–380.

Sunny, F., S. Indumati, and V. J. Daoo (2002), Preliminary measurements of aerosol optical thickness, columnar content of ozone and precipitable water at Trombay, *Bull. Indian Aerosol Sci. Technol. Assoc.*, *14*, 91–96.

Tomasi, C., S. Marani, and V. Vitale (1985), Multiwavelength Sunphotometer calibration corrected on the basis of the spectral features characterising particulate extinction and nitrogen dioxide absorption, *Appl. Opt.*, *24*, 2962–2970.

U. C. Dumka, B. Kumar, P. Pant, and R. Sagar, State Observatory, Manora Peak, Nainital, Uttaranchal 263129, India. (dumka@upso.ernet.in; brij@upso.ernet.in; ppant@upso.ernet.in; sagar@upso.ernet.in)

K. K. Moorthy, Space Physics Laboratory, Vikram Sarabhai Space Centre, Trivandrum, Kerala 695 022, India. (k-k-moorthy@eth.net)